Merging into Single-Lane Roundabouts in the Presence of Uncertainty

Ezequiel Debada and Denis Gillet

***Abstract*—Merging efficiently into roundabouts represents a challenge for autonomous vehicles due to the speed difference between merging traffic flows and the lack of certainty regarding drivers' intent, specially when the road is shared with human drivers and/or inter-vehicle communication is not available. We propose herein a strategy to merge into roundabouts, which is based on characterizing the set of merging trajectories that are safe w.r.t. the traffic on the circulatory lane and reachable by the ego vehicle. Our solution leverages the belief that some vehicles in the roundabout will exit the intersection following a non-conflicting path, and generates efficient merging trajectories without compromising safety. Moreover, our decision-making policy is formulated at a high level and does not involve explicitly generating any trajectory, whereby the required computational time remains sufficiently low. In simulation, our strategy brings benefits not only to the smoothness of the merging trajectories themselves but also to the overall traffic performance, which improves 25% w.r.t. a simpler reactive merging approach.**

I. Introduction

Autonomous vehicles (AVs) are meant to profoundly change mobility and potentially improve traffic performance and safety. Even though new Advanced Driving Assistance Systems are being deployed on commercial cars, challenges concerning autonomous driving in complex scenarios—such as traffic intersections—or understanding driver interaction and cooperation remains to be addressed in order to reach an autonomy level of 4 or higher [1]. Driving through traffic intersections is, in this respect, demanding for AVs due to the fact that coordination performance and safety heavily rely on the capacity of the motion planning strategy to make appropriate decisions in a highly dynamic and uncertain context. This is especially true in weakly-structured intersections such as roundabouts, where driving decisions are often affected by, among others, uncertainty regarding the surrounding vehicles' destinations, occluded areas, and vehicles that unexpectedly merge into the intersection.

The problem of traffic coordination at intersections has attracted a lot of attention over the last decades, and a broad range of solutions can be found in the literature [2], [3]. Among them, strategies based on vehicle-to-vehicle or vehicle-to-infrastructure communication have been shown to have the potential to improve traffic performance [4], [5], although they do not represent a valid solution for the partially connected and totally unconnected traffic scenarios AVs will face in the foreseeable future.

Concerning motion planning, two major trends are observed depending on whether maneuvers and trajectories are planned jointly (integrated approaches), or separately (modular approaches). On the one hand, integrated approaches, such as [6], [7], allow systematically addressing decision-making, but entail a high computational burden, which complicates their deployment. On the other hand, modular approaches (such as [8], [9]) represent a more practical approach that reduces computational complexity at the expense of losing optimality, yet resulting in safe and efficient decisions.

Regarding uncertainty, integrated solutions seem, however, to be favored due to the general framework they provide to handle uncertainty from different sources. For instance, solutions based on decision networks and partially-observable Markov decision processes have been recently presented in [10]–[12] and are particularly suited for situations where the surrounding obstacles' reaction to the ego vehicle's maneuver needs to be accounted for. Nonetheless, the flexibility and simplicity of modular solutions are lost and they represent an unnecessarily complex solution when the traffic regulation or the traffic dynamics itself encourages maneuvers that minimize the impact on the surrounding vehicles—as is the case of the merging maneuver at roundabouts. It is therefore reasonable in these cases to simplify the decision-making problem by considering that the surrounding vehicles' trajectories are independent of the ego vehicle's trajectory [13], [14]. Nevertheless, even when the mentioned simplification is made, very few solutions exist in the literature that handle uncertainty while still benefiting from the simplicity of a modular motion planning architecture.

Generally speaking, uncertainty constrains the ways in which a maneuver can be executed and makes necessary having a safe reaction available as long as the traffic scene cannot be sufficiently trusted. In that sense, we explore a pragmatic merging strategy for AVs at single-lane roundabouts which comprehensively handles uncertainty while allowing for a modular architecture. Inspired on the use of reachable sets for safety assessment in [15] and the trajectory planner proposed in [13], we explore a solution that characterizes the set of reachable and safe merging maneuvers without explicitly planning trajectories. Uncertainty is taken into account by only considering the merging targets that are reachable and keep available a safe reaction as long as it is necessary. Once the appropriate merging targets are identified, a multi-objective utility function is used to choose the best one.

This manuscript is organized as follows. The problem is first formalized in §II, where the assumed perception capabilities of the vehicles are as well discussed. The merging strategy is then described in §III, and the trajectory planner is formulated in §IV. Finally, simulation results are shown in §V while our conclusions are outlined in §VI.

Ezequiel Debada and Denis Gillet are with the School of Engineering at the École Polytechnique Fédérale de Lausanne (EPFL). Emails: {ezequiel.gonzalezdebada, denis.gillet } @epfl.ch

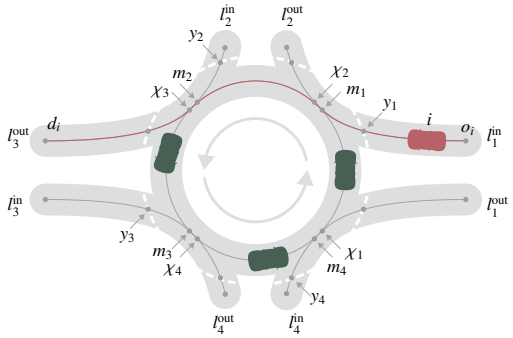

Fig. 1. Illustration of the traffic scenario studied herein.

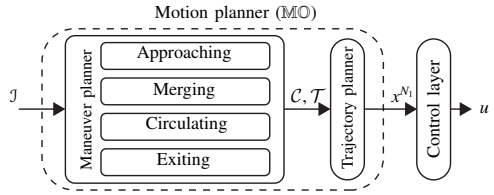

Fig. 2. Considered motion planning architecture.

II. Problem formulation.

Consider a traffic scenario (Fig. 1) where a set $\mathcal{N}$ of vehicles drive through a single-lane roundabout (SLR), modeled by the sets $\mathcal{L}_{\text{in}} = \{1, \cdots, n_{\mathcal{L}_{\text{in}}}\}$, $\mathcal{L}_{\text{out}} = \{1, \cdots, n_{\mathcal{L}_{\text{out}}}\}$, and $\mathcal{L}_{\text{cir}} = \{1\}$ of, respectively, incoming, outgoing, and circulatory lanes. Moreover, given a vehicle i, some key locations relevant for its decision-making are as well identified: the yield spot y_i, the merging spot m_i where its incoming lane intersects the circulatory lane, and the exiting spot χ_i at which its outgoing lane separate from the circulatory lane.

Vehicle $i \in \mathcal{N}$ drives along a fixed path $\pi_i(s)$ (parametrized w.r.t. the distance s driven on it) which follows the center of the lanes connecting its origin to its destination. Consequently, the vehicle's state $x_i = (s_i, v_i) \in \mathcal{X}_i$ is defined as its driven distance s_i (which along with $\pi_i(s)$ unequivocally defines its position and orientation) and speed $v_i \in \mathbb{R}_{[0,\overline{v}_i]}$ (where $\overline{v}_i$ is the maximum speed), while its control signal $u_i \in \mathcal{U}_i$ represents its longitudinal acceleration $u_i = a_i \in \mathbb{R}_{[\underline{\kappa}_i, \overline{\kappa}_i]}$ (with $\underline{\kappa}_i$ and $\overline{\kappa}_i$ being the minimum/maximum acceleration). Furthermore, the high-level information $\mathcal{I}_i \in \mathbf{I}$ the vehicle has available is assumed to contain an accurate estimation of the position and speed of all vehicles on the circulatory lane.

Regarding the AVs architecture, *motion planning* and *control* are considered to be separated (see Fig. 2) in such a way that a feasible state trajectory $x^{N_1} \in \mathcal{X}^{N_1}$ over a temporary horizon N_1 is first generated by the motion planner $\mathbb{MO} : \mathbf{I} \to \mathcal{X}^{N_1}$ given the available information, and is then followed by the control layer—which is assumed to track sufficiently well the generated trajectories. Moreover, the motion planner $\mathbb{MO}$ is considered to be divided into *maneuver planning* and *trajectory planning*.

The *maneuver planner* $\mathbb{MA} : \mathbf{I} \to \mathbf{C} \times \mathbf{T}$ performs high-level driving decisions, and outputs a set of constraints $\mathcal{C} \in \mathbf{C}$ and targets $\mathcal{T} \in \mathbf{T}$ to be considered by the trajectory planner. The set $\mathcal{C} = \{\mathcal{C}_1, \cdots, \mathcal{C}_{n_\mathcal{C}}\}$ gathers safety constraints $\mathcal{C}_i = (c_{i,\tau}, c_{i,\delta}, c_{i,v}, c_{i,d})$ (characterized by the time interval $c_{i,\tau}$ during which a safe longitudinal behavior must be kept w.r.t. an obstacle at a distance $c_{i,\delta}$ and with a speed $c_{i,v}$ by applying a deceleration $c_{i,d}$ at most). Moreover, the tuple $\mathcal{T} = \left(\mathcal{T}^V, \mathcal{T}^D\right)$ gathers a set $\mathcal{T}^V = \{\mathcal{V}_1, \cdots, \mathcal{V}_{n_\mathcal{V}}\}$ of speed targets $\mathcal{V}_i = (v_{i,\tau}, v_{i,v})$ and a set $\mathcal{T}^D = \{\mathcal{D}_1, \cdots, \mathcal{D}_{n_\mathcal{D}}\}$ of distance targets $\mathcal{D}_i = (d_{i,\tau}, d_{i,\delta})$, defining, respectively, speeds $v_{i,v}$ and distances $d_{i,\delta}$ that the vehicle should have/travel in certain time intervals $v_{i,\tau}$ and $d_{i,\tau}$. Note that, if prior knowledge of the path was not assumed, the maneuver planner output should also have included information concerning the path shape.

The *trajectory planner* $\mathbb{TR} : \mathbf{C} \times \mathbf{T} \to \mathcal{X}^{N_1}$ generates kinetically feasible state trajectories that follow the center of the lane and comply with the set of constraints and targets within $\mathcal{C} \in \mathbf{C}$ and $\mathcal{T} \in \mathbf{T}$. The task is tackled through path-velocity decomposition which, due to the path assumption described above, gets reduced to planning the speed profile v^{N_1} to follow over time.

In this paper, we study the merging maneuver at SLRs for its impact on the intersection throughout, as well as its sensitivity to uncertainty and/or imperfect information. In particular, we tackle the problem of finding a merging maneuver $\mathcal{M} = (\tau_{\text{m}}, \delta_{\text{m}}, v_{\text{m}}) \in \mathbb{R}^3$—defined by the time interval τ_{m} at which the distance δ_{m} to the merging spot needs to be reached with a merging speed v_{m}—that is reachable by the ego vehicle and safe, as well as the set of safety constraints $\mathcal{C}$ to be simultaneously imposed on the planned trajectory if further precautions were needed.

The task is carried out in a traffic context where: (i) merging maneuvers from the other incoming lanes cannot be observed or accurately predicted, (ii) the driving intent of the vehicles on the circulatory lane is unknown, and (iii) the probability with which vehicles on the circulatory lane will exit before the ego vehicle's merging spot is available.

III. Merging strategy

Broadly speaking, our approach aims at—given the distance δ_{m} to the merging spot—characterizing the set of merging targets (MTs) $\mathcal{T}_\mathcal{M} = (\tau_{\text{m}}, v_{\text{m}}) \in \mathbb{R}^2$ (tuples of merging time interval τ_{m} and merging speed v_{m}) that are safe w.r.t. the traffic in the roundabout and reachable by the ego vehicle. Our approach comprises the following steps:

1) calculating the *reachable merging targets set* $\mathcal{T}_\mathcal{M}^{\text{R}}$ containing the MTs that can be reached by the ego vehicle,
2) obtaining the set $\mathcal{G} \subseteq \mathbb{R}^2$ of gaps that can potentially be targeted, and the *safe merging targets set* $\mathcal{T}_\mathcal{M}^{\text{S}}$ of MTs that allow safely merging into every gap $\mathcal{G} \in \mathcal{G}$.
3) selecting the MT $\mathcal{T}_\mathcal{M}^*$ from the so-called *safe and reachable merging sets* $\mathcal{T}_\mathcal{M}^{\text{SR}} = \mathcal{T}_\mathcal{M}^{\text{S}} \cap \mathcal{T}_\mathcal{M}^{\text{R}}$, that maximizes the multi-objective utility function $\mathcal{Q}(\mathcal{T}_\mathcal{M})$.

The strategy is to be used in a receding horizon fashion, from the instant the ego vehicle becomes the next one on its lane to merge, up to the moment the maneuver is performed. For the sake of notation, we further consider that time and distance are expressed w.r.t. the instant at which the strategy is execute, i.e. we consider that $t_0 = 0$ and $s_0 = 0$ and that, consequently, absolute future times t and distances s are equivalent to time intervals τ and distance intervals δ.

A. Reachable sets

In this section, we begin by formulating the reachable maneuver target set (RMTS) $\mathcal{T}^{\mathrm{R}}_{\mathcal{M}}(x_0, \delta_{\mathrm{m}}) \subseteq \mathbb{R}^2$ containing all the merging targets $\mathcal{T}_{\mathcal{M}} = (\tau_{\mathrm{m}}, v_{\mathrm{m}})$ that are reachable by the ego vehicle given its current state x_0 and the maximum and minimum acceleration $\underline{\alpha}$ and $\overline{\alpha}$ to be applied). In particular, the set can be defined as

$$\begin{aligned}\mathcal{T}^{\mathrm{R}}_{\mathcal{M}}(x_0, \delta_{\mathrm{m}}) = \\ = \left\{\mathcal{T}_{\mathcal{M}} : \tau_{\mathrm{m}} \in [\underline{\tau}(\delta_{\mathrm{m}}), \overline{\tau}(\delta_{\mathrm{m}})], v_{\mathrm{m}} \in [\underline{v}(\tau_{\mathrm{m}}, \delta_{\mathrm{m}}), \overline{v}(\tau_{\mathrm{m}}, \delta_{\mathrm{m}})]\right\}, \quad (1)\end{aligned}$$

where $\underline{\tau}$ and $\overline{\tau}$ are the min/max time interval needed to drive a distance δ_{m}, and $\underline{v}$ and $\overline{v}$ are the min/max speed the vehicle can have in a time interval τ_{m} while moving forward a distance δ_{m}.

The minimum and maximum travel time required to drive a distance δ_{m} in (1) can be approximated as

$$\underline{\tau}(\delta_{\mathrm{m}}) \coloneqq \texttt{MinTT}(x_0, \delta_{\mathrm{m}}, \overline{\alpha}) = \left(-v_0 + \sqrt{v_0^2 + 2\overline{\alpha}\delta_{\mathrm{m}}}\right)/\overline{\alpha}\ , \quad (2)$$

$$\overline{\tau}(\delta_{\mathrm{m}}) \coloneqq \texttt{MaxTT}(x_0, \delta_{\mathrm{m}}, \underline{\alpha}) = \begin{cases}\texttt{MinTT}(x_0, \delta_{\mathrm{m}}, \underline{\alpha}) & \text{if } v_0 \geq \texttt{MSS}(\delta_{\mathrm{m}}, -\underline{\alpha}) \\ \infty & \text{otherwise}\end{cases}, \quad (3)$$

where the auxiliary function $\texttt{MSS} : \mathbb{R}^2 \to \mathbb{R}^1$, defined as

$$\texttt{MSS}(\delta_{\mathrm{m}}, d) = \sqrt{2d\delta_{\mathrm{m}}}\ , \quad (4)$$

returns the maximum safe speed (MSS) that allows fully braking in less than a distance δ_{m} with deceleration d.

Then, letting T be a certain time step, and denoting a discrete-time state and control input trajectory over N time steps as x^N, u^N, the boundaries $\underline{v}$ and $\overline{v}$ can be calculated by solving, given δ_{m} and for all $\tau_{\mathrm{m}} \in [\underline{\tau}, \overline{\tau}]$) the set of linear programs (LPs)

$$\underline{v} = \min_{x^N, u^N}\{v(N) : \mathcal{C}_{\mathrm{LP}}\}\ , \qquad \overline{v} = \max_{x^N, u^N}\{v(N) : \mathcal{C}_{\mathrm{LP}}\}\ , \quad (5)$$

with $N = \lceil \tau_{\mathrm{m}}/T \rceil$ and subject to the set of constraints

$$\begin{aligned}\mathcal{C}_{\mathrm{LP}} = \{\ & s(k+1) = s(k) + v(k)T + 0.5u(k)T^2 && \forall k \in [0, N-1], \quad (6)\\ & v(k+1) = v(k) + u(k)T && \forall k \in [0, N-1], \quad (7)\\ & v(k) \in [0, \overline{v}], \quad u(k) \in [\underline{\alpha}, \overline{\alpha}] && \forall k \in [0, N-1], \quad (8)\\ & s(0) = 0, \quad v(0) = v_0, \quad s(N) = \delta_{\mathrm{m}}\ \}\ . && (9)\end{aligned}$$

Specifically, (6)–(7) impose the considered longitudinal motion model, (8) sets the range of values for the decision variables, and (9) imposes the initial and terminal conditions.

Assessing the solutions of (5) it can be concluded that:

1) the optimal trajectory turns out to be, as long as the rendered speed trajectory does not violate the minimum and maximum speed constraint, the one given by the acceleration profile

$$u(\tau) = \begin{cases} a_1 & \text{if } 0 \leq \tau \leq \tau_1 \\ a_2 & \text{if } \tau_1 < \tau \leq \tau_{\mathrm{m}}\end{cases} \quad (10)$$

with (a_1, a_2) being $(\underline{\alpha}, \overline{\alpha})$ for $\overline{v}(\tau_{\mathrm{m}})$ and $(\overline{\alpha}, \underline{\alpha})$ for $\underline{v}(\tau_{\mathrm{m}})$, and τ_1 taking the value that allows traveling a distance δ_{m}.

2) concerning the minimum merging speed $\underline{v}(\tau_{\mathrm{m}}, \delta_{\mathrm{m}})$, the previous acceleration profile leads to the boundary value for all merging times up to $\tau_{\mathrm{m}} = \tau_2$, which is the minimum merging time at which $v(\tau_{\mathrm{m}}) = 0$. From that instant on, the lower boundary always takes value 0.

3) similarly, the value of the maximum merging speed $\overline{v}(\tau_{\mathrm{m}}, \delta_{\mathrm{m}})$ results from (10) up to the merging time interval $\tau_{\mathrm{m}} = \tau_3$, for which the speed at time τ_1 (when the acceleration changes its value) is $v(\tau_1) = 0$. From that time on, the maximum merging speed becomes constant as well.

These points can be exploited to find the analytical expression of $\underline{v}(\tau_{\mathrm{m}}, \delta_{\mathrm{m}})$ and $\overline{v}(\tau_{\mathrm{m}}, \delta_{\mathrm{m}})$.

Let us begin by writing the evolution of the state over time given (10), that is

$$v(\tau) = \begin{cases} v_0 + a_1\tau & \text{if } 0 \leq \tau \leq \tau_1 \\ v(\tau_1) + a_2(\tau - \tau_1) & \text{if } \tau_1 < \tau \leq \tau_{\mathrm{m}}\end{cases}\ , \quad (11)$$

$$s(\tau) = \begin{cases} v_0\tau + \frac{a_1\tau^2}{2} & \text{if } 0 \leq \tau \leq \tau_1 \\ s(\tau_1) + \frac{\Delta a(\tau - \tau_1)^2}{2} & \text{if } \tau_1 < \tau \leq \tau_{\mathrm{m}}\end{cases}\ , \quad (12)$$

with $\Delta a = a_2 - a_1$. Then, imposing $s(\tau_{\mathrm{m}}) = \delta_{\mathrm{m}}$ in (12) we can obtain the time interval

$$\tau_1 = \tau_{\mathrm{m}} - \sqrt{\left(2\delta_{\mathrm{m}} - 2v_0\tau_{\mathrm{m}} - a_1\tau_{\mathrm{m}}^2\right)/\Delta a} \quad (13)$$

at which the acceleration must change its value to travel a distance δ_{m}.

Moreover, by substituting (13) in (11), the expression

$$\begin{aligned}v(\tau_{\mathrm{m}}, \delta_{\mathrm{m}}) = \texttt{TS}(\tau_{\mathrm{m}}, \delta_{\mathrm{m}}, v_0, a_1, a_2) = \\ = v_0 + a_1\tau_{\mathrm{m}} + \sqrt{\Delta a\left(2\delta_{\mathrm{m}} - 2v_0\tau_{\mathrm{m}} - a_1\tau_{\mathrm{m}}^2\right)} \quad (14)\end{aligned}$$

for the terminal speed (TS) can be obtained, which shapes the segment of $\underline{v}(\cdot)$ and $\overline{v}(\cdot)$ up to, respectively, τ_2 and τ_3.

Subsequently, the time interval τ_2 at which the value of the lower boundary becomes constant can be calculated as

$$\tau_2 = \begin{cases} \frac{-\underline{\alpha}v_0 - \sqrt{\underline{\alpha}^2v_0^2 - \underline{\alpha}\overline{\alpha}\left(v_0^2 + 2\delta_{\mathrm{m}}(\overline{\alpha} - \underline{\alpha})\right)}}{\underline{\alpha}\overline{\alpha}} & \text{if } v_0 \leq \texttt{MSS}(\delta_{\mathrm{m}}, -\underline{\alpha}) \\ \overline{\tau}(\delta_{\mathrm{m}}) & \text{otherwise}\end{cases}, \quad (15)$$

i.e., the time τ_2 at which $v(\tau_2) = 0$ in (14) with $(a_1, a_2) = (\overline{\alpha}, \underline{\alpha})$ if the vehicle can stop before δ_{m}, or the maximum travel time interval $\overline{\tau}(\delta_{\mathrm{m}})$ needed to reach the spot otherwise.

Likewise, the upper boundary becomes constant from the merging time

$$\tau_3 = \begin{cases} \frac{-\overline{\alpha}v_0 - \sqrt{\overline{\alpha}\left(\underline{\alpha}v_0^2 + 2\underline{\alpha}^2\delta_{\mathrm{m}}\right)}}{\overline{\alpha}\underline{\alpha}} & \text{if } v_0 \leq \texttt{MSS}(\delta_{\mathrm{m}}, -\underline{\alpha}) \\ \overline{\tau}(\delta_{\mathrm{m}}) & \text{otherwise}\end{cases}\ , \quad (16)$$

i.e., the one for which $v(\tau_1) = 0$ in (11) with $(a_1, a_2) = (\underline{\alpha}, \overline{\alpha})$ if the vehicle has enough space to brake before δ_{m}, or the maximum time interval $\overline{\tau}(\delta_{\mathrm{m}})$ to reach the spot otherwise.

Consequently, the boundaries $\underline{v}(\tau_{\mathrm{m}})$ and $\overline{v}(\tau_{\mathrm{m}})$ are

$$\underline{v}(\tau_{\mathrm{m}}, \delta_{\mathrm{m}}) = \begin{cases} \texttt{TS}(\tau_{\mathrm{m}}, \delta_{\mathrm{m}}, v_0, \overline{\alpha}, \underline{\alpha}) & \text{if } \underline{\tau}(\delta_{\mathrm{m}}) \leq \tau_{\mathrm{m}} \leq \tau_2 \\ 0 & \text{if } \tau_2 < \tau \leq \overline{\tau}(\delta_{\mathrm{m}})\end{cases}\ , \quad (17)$$

$$\overline{v}(\tau_{\mathrm{m}}, \delta_{\mathrm{m}}) = \begin{cases} \texttt{TS}(\tau_{\mathrm{m}}, \delta_{\mathrm{m}}, v_0, \underline{\alpha}, \overline{\alpha}) & \text{if } \underline{\tau}(\delta_{\mathrm{m}}) \leq \tau_{\mathrm{m}} \leq \tau_3 \\ \texttt{TS}(\tau_3, \delta_{\mathrm{m}}, v_0, \underline{\alpha}, \overline{\alpha}) & \text{if } \tau_3 < \tau \leq \overline{\tau}(\delta_{\mathrm{m}})\end{cases}\ , \quad (18)$$

which along with (2) and (3), provide an analytical way of building the set (1).

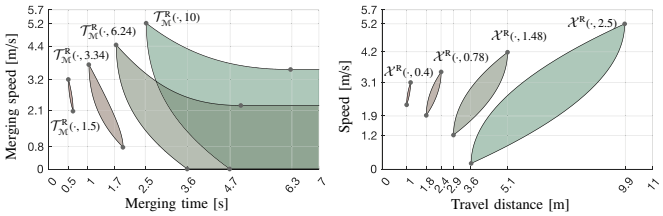

Fig. 3. Reachable merging targets sets $\mathcal{T}^{\mathrm{R}}_{\mathcal{M}}$ (left hand side) and reachable states sets $\mathcal{X}^{\mathrm{R}}$ for a vehicle with $x_0 = (0, 2.7)$, $\underline{\alpha} = -1$ m/s^2, $\overline{\alpha} = 1$ m/s^2, and different values of δ_{m} and τ_{m}.

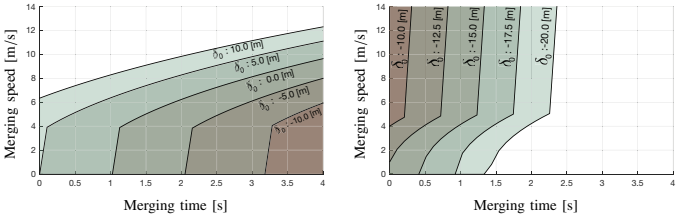

Fig. 4. Safe merging targets sets to merge after a leading vehicle (left-hand side plot) and before a following vehicle (right-hand side plot), positioned at different distances δ_0 from the merging spot.

From this derivation, one can as well obtain the reachable states set (RSS)

$$\mathcal{X}^{\mathrm{R}}(x_0, \tau') = \left\{(\delta, v) : (\tau', v) \in \mathcal{T}^{\mathrm{R}}_{\mathcal{M}}(x_0, \delta)\right\} \tag{19}$$

containing the states that can be reached by the ego vehicle in a time interval τ' (see Fig. 3 for some samples of RSSs as well as RMTSs).

B. Merging gaps

The next step consists of identifying the gaps $\mathcal{G} = (g_{\mathrm{L}}, g_{\mathrm{F}})$, defined by a leading vehicle g_{L} and a following vehicle g_{F}, that will be considered to accommodate the merging maneuver. Particularly, the set of potential merging gaps to consider can be built as

$$\mathcal{G}(t) = \left\{(g_{\mathrm{L}}, g_{\mathrm{F}}) : g_{\mathrm{L}}, g_{\mathrm{F}} \in \mathcal{N}', \delta^{m_{\mathrm{ego}}}_{g_{\mathrm{F}}} \geq \delta^{m_{\mathrm{ego}}}_{g_{\mathrm{L}}}\right\}. \tag{20}$$

where $\mathcal{N}'$ denotes a certain set of vehicles on the circulatory lane, and $\delta^{m_{\mathrm{ego}}}_{g_k}$ is the distance from vehicle g_k to the ego vehicle's merging spot m_{ego}.

The state of the gap is denoted as $x_{\mathcal{G}} = (x_{g_{\mathrm{L}}}, x_{g_{\mathrm{F}}}, \mathrm{P}^{\mathrm{e}}_{\mathcal{G}}, \tau^{\mathrm{e}}_{\mathcal{G}})$ and it contains the states $x_{g_{\mathrm{L}}}$, $x_{g_{\mathrm{F}}}$ of, respectively, the leading and following vehicles, the probability $\mathrm{P}^{\mathrm{e}}_{\mathcal{G}}$ with which the gap $\mathcal{G}$ is expected to arrive empty at the merging spot, and the discovery time interval $\tau^{\mathrm{e}}_{\mathcal{G}}$ at which this uncertainty is expected to vanish. Letting $\mathcal{N}_{\mathcal{G}} \subseteq \mathcal{N}'$ be the subset of vehicles in $\mathcal{N}'$ that are positioned between vehicles g_{L} and g_{F}, $\mathrm{P}^{\mathrm{c}}_i$ denote the probability that a vehicle i follows a conflicting path, and

$$\tau^{\mathrm{e}}_i = \mathtt{MaxTT}\left(x_i, \overline{\delta}^{\mathcal{N}}_i, d^{\mathrm{u}}_i\right), \tag{21}$$

be the time interval at which vehicle i will have the last chance to exit the roundabout before the ego vehicle's merging spot (with $\overline{\delta}^{\mathcal{N}}_i$ being the distance from vehicle i to its furthest exit before m_{ego} and assuming vehicle i applies an average deceleration d^{u}_i over time), the existence probability and discovery time of a gap are calculated as

$$\mathrm{P}^{\mathrm{e}}_{\mathcal{G}} = \begin{cases} 1 & \text{if } \mathcal{N}_{\mathcal{G}} = \emptyset \\ \prod_{i \in \mathcal{N}_{\mathcal{G}}} (1 - \mathrm{P}^{\mathrm{c}}_i) & \text{otherwise} \end{cases} \quad \text{and} \quad \tau^{\mathrm{e}}_{\mathcal{G}} = \max_{i \in \mathcal{N}_{\mathcal{G}}} \tau^{\mathrm{e}}_i. \tag{22}$$

Consequently, gaps will be from now on referred to as *certain* if $\mathrm{P}^{\mathrm{e}}_{\mathcal{G}} = 1$, and *uncertain* otherwise.

At this point, we propose a construction of the set of vehicles $\mathcal{N}'$ which will naturally lead to merging maneuvers that are safe w.r.t. unexpected vehicles merging from other incoming lanes. Particularly, the set $\mathcal{N}' = \mathcal{N}_{\mathrm{c}} \cup \mathcal{W}_{\mathrm{c}}$ will be constructed as the set $\mathcal{N}_{\mathrm{c}}$ of circulating vehicles, extended with a set $\mathcal{W}_{\mathrm{c}} = \{w_i : i \in [1, n_{\mathcal{L}_{\mathrm{in}}}]\}$ of auxiliary virtual vehicles. Vehicles within $\mathcal{W}_{\mathrm{c}}$ will be positioned at the merging spots of the surrounding incoming lanes, to make the maneuver planner select merging targets that are appropriate even if a vehicle unexpectedly merges to the circulatory lane. To fully characterize the auxiliary virtual vehicles, they are as well assigned a certain speed $v_{w_i} = \omega$, and conflicting probability $\mathrm{P}^{\mathrm{c}}_{w_i} = \epsilon$.

C. Safe merging sets

For every observed gap $\mathcal{G} \in \mathcal{G}$, we aim to calculate the safe merging targets set (SMTS)

$$\mathcal{T}^{\mathrm{S}}_{\mathcal{M}}(x_0, x_{\mathcal{G}}, \delta_{\mathrm{m}}) = \mathcal{T}^{\mathrm{SL}}_{\mathcal{M}}(x_{g_{\mathrm{L}}}, \delta_{\mathrm{m}}) \cap \mathcal{T}^{\mathrm{SF}}_{\mathcal{M}}(x_{g_{\mathrm{F}}}, \delta_{\mathrm{m}}) \cap \mathcal{T}^{\mathrm{SU}}_{\mathcal{M}}(x_0, x_{\mathcal{G}}, \delta_{\mathrm{m}}) \tag{23}$$

gathering the MTs that allow safely merging in the gap. Specifically, it is constructed as the intersection of the sets $\mathcal{T}^{\mathrm{SL}}_{\mathcal{M}}$ and $\mathcal{T}^{\mathrm{SF}}_{\mathcal{M}}$ (containing the safe MTs to merge after vehicle g_{L} and before g_{F}, respectively) as well as the set $\mathcal{T}^{\mathrm{SU}}_{\mathcal{M}}$ gathering the MTs that are safe w.r.t. the gap appearance uncertainty.

Before tackling the construction of such sets, let us introduce for the sake of notation, the auxiliary set

$$\mathcal{X}^{\mathrm{SCF}}(x_L) = \left\{x_F : (s_L - s_F) > v_F \Theta_F + 0.5\left(v_F^2 - v_L^2\right)/d\right\} \tag{24}$$

gathering—given the state x_L of a vehicle L—the states x_F that would allow a vehicle F to safely drive behind it, with Θ_F being the reaction time of the follower vehicle and assuming both cars can apply the same maximum deceleration d [16]).

a) SMTS w.r.t. leading and following vehicles: The SMTS to merge after/before the leading/following vehicle can be written as

$$\mathcal{T}^{\mathrm{SL}}_{\mathcal{M}}(x_{g_{\mathrm{L}}}, \delta_{\mathrm{m}}) = \left\{\mathcal{T}_{\mathcal{M}} : (\delta_{\mathrm{m}}, v) \in \mathcal{X}^{\mathrm{SCF}}(\hat{x}_L(\tau))\right\}, \tag{25}$$

$$\mathcal{T}^{\mathrm{SF}}_{\mathcal{M}}(x_{g_{\mathrm{F}}}, \delta_{\mathrm{m}}) = \left\{\mathcal{T}_{\mathcal{M}} : \hat{x}_F(\tau) \in \mathcal{X}^{\mathrm{SCF}}((\delta_{\mathrm{m}}, v))\right\}, \tag{26}$$

i.e., as the set of MTs that lead to a safe car-following situation for the ego vehicle w.r.t. the leading vehicle, and for the following vehicle w.r.t. the ego vehicle. In (25)-(26), $\hat{x}_L(\tau)$ and $\hat{x}_F(\tau)$ represent the estimated state of vehicles L and F after a time interval τ, which are approximated by

$$\hat{s}_k(\tau) = \delta^{m_{\mathrm{ego}}}_{\mathrm{ego}} - \delta^{m_{\mathrm{ego}}}_k(0) + v_k(0)\tau + 0.5\hat{a}_k\tau^2, \tag{27}$$

$$\hat{v}_k(\tau) = v_k(0) + a_k\tau, \tag{28}$$

for all $k = \{L, F\}$, assuming they apply—on average—the acceleration a_k, which can be tuned to control the level of conservativeness wanted on the estimation.

Some examples of the safe MTs sets w.r.t. the leading and following vehicles resulting from this method can be seen in Fig. 4.

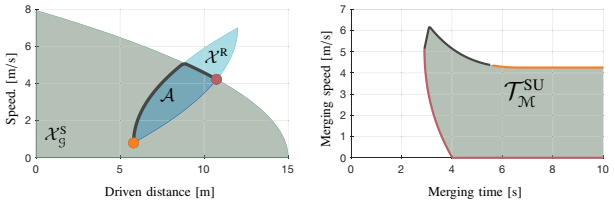

Fig. 5. SMTS (right-hand side plot) and intermediary sets involved in its construction (left-hand side plot), for a vehicle with $v_0 = 5$ m/s, $\delta_{\mathrm{m}} = 15$ m, willing to decelerate at $d = 2$ m/s^2 to abort its merging maneuver, and wanting to stay at a safe braking distance from the merging spot during the following $\tau^{\mathrm{e}} = 2$ s.

b) SMTS w.r.t. gap uncertainty: Characterizing the SMTS $\mathcal{T}^{\mathrm{SU}}_{\mathcal{M}}$ w.r.t. the gap uncertainty requires isolating the MTs that allow safely braking before the yield line y_{ego} at least during the time $\tau^{\mathrm{e}}_{\mathcal{G}}$. This means that, unlike $\mathcal{T}^{\mathrm{SL}}_{\mathcal{M}}$ and $\mathcal{T}^{\mathrm{SF}}_{\mathcal{M}}$, which contain the MTs that allow *safely merging* in the gap w.r.t. vehicles g_{L} and g_{F}, the set $\mathcal{T}^{\mathrm{SU}}_{\mathcal{M}}$ gathers the MTs that allow *safely approaching* the gap being evaluated.

The construction of $\mathcal{T}^{\mathrm{SU}}_{\mathcal{M}}$ is tackled in two stages: we first identify the set of safe approaching states, i.e. those that can be reached in a time $\tau^{\mathrm{e}}_{\mathcal{G}}$ and allow braking before the yield line, and then aggregate the RMTS from all those states.

Let us begin by introducing the maximum deceleration $d^{\mathrm{c}}_{\mathcal{G}}$ the ego vehicle will be willing to apply if it had to abort a merging maneuver that relies on the appearance of an uncertain gap $\mathcal{G}$. We consider $d^{\mathrm{c}}_{\mathcal{G}}$ to be dependent on the existence probability the ego vehicle assigns to the gap, in such a way that the more confident it is about the materialization of the gap, the higher the deceleration it is willing to apply. Specifically, the linear correlation

$$d^{\mathrm{c}}_{\mathcal{G}} = d^{\mathrm{stop}} + \Delta d \mathrm{P}^{\mathrm{e}}_{\mathcal{G}} \tag{29}$$

is proposed, where d^{stop} is the deceleration that ego would apply to gently stop at the yield line, and $\Delta d \geq 0$ represents how much harder it would be willing to decelerate if the gap ends up not appearing despite his high level of confidence.

Then, denoting the state of the obstacle representing the yield line as $x_y = (s_0 + \delta^y_{\mathrm{ego}}, 0)$, we can construct the set

$$\mathcal{A}(x_0, \tau) = \mathcal{X}^{\mathrm{R}}(x_0, \tau) \cap \mathcal{X}^{\mathrm{SCF}}(x_y) \tag{30}$$

of reachable states that allow stopping before the yield line placed at a distance δ^y_{ego}.

Once such a set is obtained, the set of MTs that can be safely approached can be built as

$$\mathcal{T}^{\mathrm{SU}}_{\mathcal{M}}(x_0, x_{\mathcal{G}}, \delta_{\mathrm{m}}) = \\ = \begin{cases} \mathcal{T}^{\mathrm{R}}_{\mathcal{M}}(x_0, \delta_{\mathrm{m}}) & \text{if } \mathrm{P}^{\mathrm{e}}_{\mathcal{G}} = 1 \\ (\tau^{\mathrm{e}}_{\mathcal{G}}, 0) + \bigcup_{x' \in \mathcal{A}(x_0, \tau^{\mathrm{e}}_{\mathcal{G}})} \mathcal{T}^{\mathrm{R}}_{\mathcal{M}}(x', \delta_{\mathrm{m}} - s') & \text{otherwise} \end{cases}, \tag{31}$$

where the union of the RMTS from the states within $\mathcal{A}(x_0, \tau^{\mathrm{e}}_{\mathcal{G}})$ has been shifted $\tau^{\mathrm{e}}_{\mathcal{G}}$ in time, to account for the fact that those reachable MTs are calculated w.r.t. the reachable states at the time of discovery.

Experimentally, it has been observed that the resulting $\mathcal{T}^{\mathrm{SU}}_{\mathcal{M}}$ uniquely depends on the upper boundary of $\mathcal{A}(x_0, \tau^{\mathrm{e}}_{\mathcal{G}})$, which could be calculated as

$$\overline{\mathcal{A}}(x_0, \tau^{\mathrm{e}}_{\mathcal{G}}) = \left\{(s, \overline{v}) : \overline{v} \geq v, (s, v) \in \mathcal{A}(x_0, \tau^{\mathrm{e}}_{\mathcal{G}})\right\}, \tag{32}$$

allowing its direct substitution in (31). This practical aspect (illustrated in Fig. 5), along with the analytical expression for the set of reachable states, can be exploited for an efficient implementation. In Fig. 5 the intermediary sets used in the construction of $\mathcal{T}^{\mathrm{SU}}_{\mathcal{M}}$, and the set itself are shown. Furthermore, the upper boundary $\overline{\mathcal{A}}$ and some of its key points have been highlighted, along with the segments of the boundary of $\mathcal{T}^{\mathrm{SU}}_{\mathcal{M}}$ that they are responsible for.

D. Decision and maneuver planner output

The intersection between the RMTS $\mathcal{T}^{\mathrm{R}}_{\mathcal{M}}(x_0, \delta_{\mathrm{m}})$, and the set SMTS $\mathcal{T}^{\mathrm{S}}_{\mathcal{M}}(x_0, x_{\mathcal{G}}, \delta_{\mathrm{m}})$, results in the set

$$\mathcal{M}_{\mathcal{G}} \coloneqq \mathcal{T}^{\mathrm{SR}}_{\mathcal{M}}(x_0, x_{\mathcal{G}}, \delta_{\mathrm{m}}) = \mathcal{T}^{\mathrm{S}}_{\mathcal{M}}(x_0, x_{\mathcal{G}}, \delta_{\mathrm{m}}) \cap \mathcal{T}^{\mathrm{R}}_{\mathcal{M}}(x_0, \delta_{\mathrm{m}}), \tag{33}$$

of all candidate MTs that are reachable and safe w.r.t. each gap $\mathcal{G}$. The only step remaining is to choose a specific MT to pursue from within the sets.

We propose selecting the MT by doing

$$\mathcal{T}^*_{\mathcal{M}} = \arg\max_{\mathcal{T}_{\mathcal{M}}} \{\mathcal{Q}(\mathcal{T}_{\mathcal{M}}) : \mathcal{T}_{\mathcal{M}} \in \cup_{\mathcal{G} \in \mathcal{G}} \mathcal{M}_{\mathcal{G}}\}, \tag{34}$$

with $\mathcal{Q}(\mathcal{T}_{\mathcal{M}}) : \mathbb{R}^2 \to \mathbb{R}$ being a function assigning a quality score to every merging target.

The design of $\mathcal{Q}$ could vary depending on the purpose. It is worth noting however that while characterizing the RMTS and SMTSs, safety and feasibility aspects were already considered, and therefore they do not need to be accounted for in the scoring function. Consequently, a rather simple scoring function is considered herein, which takes the form

$$\mathcal{Q}(\mathcal{T}_{\mathcal{M}}) = \omega_\tau \tau_{\mathrm{m}} + \omega_v v_{\mathrm{m}} + \omega_{\mathrm{P}} \mathrm{P}^{\mathrm{s}}_{\mathcal{T}_{\mathcal{M}}}. \tag{35}$$

That is, the weighted sum of the merging time and speed, and the probability $\mathrm{P}^{\mathrm{s}}_{\mathcal{T}_{\mathcal{M}}}$ of succeeding at merging by pursuing the MT $\mathcal{T}_{\mathcal{M}}$. Specifically, noting that if a MT lies within the set of safe MTs w.r.t. several gaps is because they share some portion of the road—and therefore their appearance events are dependent—the merging success probability of a MT would be equivalent to the existence probability of the most probable gap it belongs to. Specifically, letting

$$\mathcal{G}^*(\mathcal{T}_{\mathcal{M}}) = \arg\max_{\mathcal{G} \in \mathcal{G}} \left\{\mathrm{P}^{\mathrm{e}}_{\mathcal{G}} \mathbf{1}_{\mathcal{S}_{\mathcal{G}}}(\mathcal{T}_{\mathcal{M}})\right\} \tag{36}$$

denote (with $\mathbf{1}$ being the indicator function) the most probable gap a certain MT belongs to, $\mathrm{P}^{\mathrm{s}}_{\mathcal{T}_{\mathcal{M}}}$ in (35) would be $\mathrm{P}^{\mathrm{s}}_{\mathcal{T}_{\mathcal{M}}} = \mathrm{P}^{\mathrm{e}}_{\mathcal{G}^*(\mathcal{T}_{\mathcal{M}})}$.

a) Maneuver planner output: The chosen MT $\mathcal{T}^*_{\mathcal{M}}$, along with the current distance δ_{m} to the merging spot, lead to the high-level merging maneuver $\mathcal{M} = (\tau^*, v^*, \delta_{\mathrm{m}})$ which will be passed to the trajectory planner as the pair of targets $\mathcal{T}^V = \{(\tau^*, v^*)\}$ and $\mathcal{T}^D = \{(\tau^*, \delta_{\mathrm{m}})\}$.

Moreover, the set $\mathcal{C} = \{\mathcal{C}_1\}$ of trajectory constraints complementing the MT is calculated as

$$\mathcal{C}_1 = \begin{cases} \emptyset & \text{if } \mathrm{P}^{\mathrm{e}}_{\mathcal{G}^*(\mathcal{T}_{\mathcal{M}})} = 1 \\ \left(\tau^{\mathrm{e}}_{\mathcal{G}^*(\mathcal{T}^*_{\mathcal{M}})}, \delta^y_{\mathrm{ego}}, 0, d^{\mathrm{c}}_{\mathcal{G}^*(\mathcal{T}^*_{\mathcal{M}})}\right) & \text{otherwise} \end{cases}. \tag{37}$$

That is, it is empty if the chosen MT targets a certain gap, and otherwise expresses a safety constraint w.r.t. the yield line as long as the gap remains uncertain.

IV. Trajectory planner

The trajectory planner follows the path-velocity decomposition approach, i.e. an appropriate path is first planned, and then the velocity profile with which it should be followed is obtained. The path is here considered to be unequivocally given by the roundabout layout, the vehicle's origin and the targeted destination, whereas the velocity profile will be planned using a quadratic program (QP) that takes into account the set $\mathcal{T}^V$, $\mathcal{T}^D$ of targets, and the set $\mathcal{C}$ of safety constraints.

Particularly, letting T show the sampling time, and the auxiliary function $\mathtt{K}(\tau) = \lfloor \tau/T \rfloor$ return the time step corresponding to a time interval τ, the speed profile to pursue over N_1 time steps is obtained from

$$\left(u^{N_1}{}^*, x^{N_1}{}^*\right) = \arg\min_{u^{N_1}, x^{N_1}} \left\{ \mathcal{J}\left(u^{N_1}{}^*, x^{N_1}{}^*\right) : \mathcal{C}_{\mathrm{QP}} \right\}, \tag{38}$$

where the cost function is formulated as

$$\begin{aligned}\mathcal{J}(\cdot) =& \omega_{\mathcal{D}} \sum_{i=1}^{n_{\mathcal{D}}} \Delta s_i^2(\mathtt{K}(d_{i,\tau})) + \\ &+ \omega_{\mathcal{V}} \sum_{i=1}^{n_{\mathcal{V}}} \Delta v_i^2(\mathtt{K}(v_{i,\tau})) + \sum_{k=1}^{N} \omega_{\mathrm{u}} u^2(k) - \omega_{\mathrm{v}} v^2(k) \,,\end{aligned} \tag{39}$$

with $\Delta s_i(\cdot) = (s(\cdot) - d_{i,s})$, and $\Delta v(\cdot) = (v(\cdot) - v_{i,v})$ being the position and speed deviation w.r.t. the targets (weighted with $\omega_{\mathcal{D}}$ and $\omega_{\mathcal{V}}$), and terms $\omega_{\mathrm{u}} u^2(\cdot)$ and $\omega_{\mathrm{v}} v^2(\cdot)$ accounting for trajectory smoothness and speed.

Moreover, the set $\mathcal{C}_{\mathrm{QP}}$ in (38) gathers the constraints

$$s(k+1) = s(k) + v(k)T + 0.5u(k)T^2, \ k \in [0, N-1], \tag{40}$$

$$v(k+1) = v(k) + u(k)T, \ k \in [0, N-1], \tag{41}$$

$$2c_{i,d}(c_{i,\delta} + c_{i,v}k'T - s(k')) + c_{i,v}^2 \geq v^2(k'), \ i \in [1, n_{\mathcal{C}}], k' \leq \mathtt{K}(c_{i,\tau}) \tag{42}$$

$$v(k) \in [0, \overline{v}], \quad u(k) \in [\underline{\kappa}, \overline{\kappa}], \ k \in [0, N-1], \tag{43}$$

$$s(0) = 0, \ v(0) = v_0, \ a(0) = a_0, \tag{44}$$

where (40)–(41) implement the motion model, (42) imposes the safety constraint, (43) defines the valid range of values of the decision variables, and (44) sets the initial conditions.

Constraint (42) is nonlinear but convex, hence it can be approximated by a set of linear inequalities. In particular, selecting a set of speed values $\mu = \left\{\mu_1, \mu_2, \cdots, \mu_{n_\mu}\right\}$ conveniently distributed within the range $[\underline{v}, \overline{v}]$, (42) can be approximated as the set of inequalities

$$2c_{i,d}(c_{i,\delta} + c_{i,v}kT - s(k)) + c_{i,v}^2 \geq 2\mu_j v(k) - \mu_j^2 \tag{45}$$

for all $j \in [1, n_\mu]$.

V. Results

In this section, several aspects of the proposed algorithm are assessed. We start by showing the computational time required by our implementation. Then, the high-level decision-making and merging strategies are qualitatively analyzed and illustrated. Finally, we run a large batch of simulations and compare the overall traffic coordination performance resulting from the proposed strategy w.r.t. a baseline reactive merging policy, and a variation of the proposed behavior that does not take into account uncertain gaps.

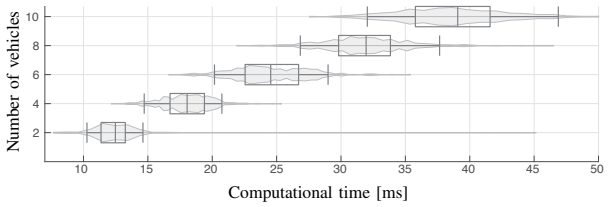

Fig. 6. Computational time required by the maneuver planner to obtain a solution, for different number of vehicles on the circulatory lane.

The results presented in this section were obtained for the following parameters values: $\overline{v} = 30$ m/s, $\underline{\kappa} = -6$ m/s^2, $\overline{\kappa} = 4$ m/s^2, $\overline{\alpha} = 2$ m/s^2, $\underline{\alpha} = 3$ m/s^2, $\omega = 1$, $\epsilon = .1$, $d^{\mathrm{u}} = .1$ m/s^2, $d^{\mathrm{l}} = .3$ m/s^2, $d^{\mathrm{stop}} = .1$ m/s^2, $\Delta d = .2$ m/s^2, $\Theta_{\mathrm{ego}} = .01$ s, $\Theta_{\mathrm{f}} = .5$ s, $\omega_\tau = -70$ 1/s, $\omega_v = 10$ s/m, $\omega_{\mathrm{P}} = 2.5$, $N_1 = 25$ s, $T = .1$ s, $\omega_{\mathcal{D}} = 50$ 1/m, $\omega_{\mathcal{V}} = 150$ s/m, $\omega_{\mathrm{u}} = 10$ s^2/m, $\omega_{\mathrm{v}} = 1$ s/m, $n_\mu = 10$, $\hat{a}_{g_{\mathrm{F}}} = .3$, $\hat{a}_{g_{\mathrm{L}}} = -.3$. It is worth noting that the presented values were manually tuned, and that slightly different behaviors (and probably more efficient ones) can be obtained by optimizing this process—which is out of the scope of this article.

A. Computational time

The time it takes our Matlab implementation of the proposed maneuver planner to obtain a solution—on an iMac i7 4.2Ghz, 64Gb RAM—is shown in Fig. 6 w.r.t. the number of vehicles on the circulatory lane. As it can be seen, the algorithm is fast and the computational time grows roughly linearly with the number of vehicles within the intersection.

Every distribution represented by box plots in Fig. 6 contains 1k samples obtained from the application of the algorithm to a series of fabricated traffic scenes. Moreover, it is worth noting that one could always set a maximum number of gaps to be considered by the algorithm in order to upper bound the computational time, at the expense of a potential loss of performance.

B. Decision making

The main benefit of the proposed maneuver planner can be visualized in Fig. 7. Therein, two examples of traffic scenes are depicted. For each of them, we show the resulting non-empty safe and reachable merging targets sets if (case 1) the algorithm only considered certain gaps, and (case 2) if both certain and uncertain gaps were accounted for. This comparison aims at evaluating the impact the explicit treatment of uncertainty has on the merging decision.

In case 1 the algorithm would make the vehicle considers feasible only the merging option consisting of waiting for all vehicles to pass, and then merge after the last one. On the contrary, the explicit consideration of uncertainty concerning the surrounding vehicles intent in case 2, would allow safely pursuing a merging option that is potentially better, yet uncertain.

Something to be noted is that some portions of the sets overlap with each other—see for instance merging sets $\mathcal{M}_{1,3}$ and $\mathcal{M}_{1,\infty}$ in example 2 case-2—which is a direct consequence of the fact that uncertain gaps can overlap.

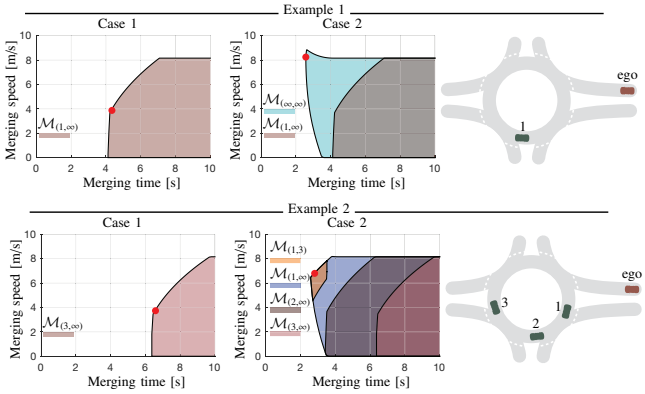

Fig. 7. Illustration of the proposed maneuver planner. Two examples are shown, each one corresponding to a certain traffic scene shown on the right hand side. The plots show the resulting non-empty safe and reachable merging targets sets in case only certain gaps were considered (case 1), and if uncertain gaps were as well taken into account (case 2). The red dots represent the optimal MT that would be chosen by the algorithm.

C. Merging trajectories

The quality of the merging trajectories is as well affected by the changes on the decision-making strategy as can be observed in Fig. 8. Similarly to what was done in §V-B, the merging trajectories shown therein were obtained by running the same traffic scenario twice: the first time (case 1) the algorithm was forced to only consider certain gaps, while in the second run (case 2) uncertain gaps were as well included. Furthermore, in case 2, vehicles are assumed to guess the right destination of the vehicles with 90% confidence.

Qualitatively speaking, collisions were avoided in both cases, and in case 2 the merging trajectories were smoother and allowed most of the incoming vehicles to merge earlier to the roundabout.

Firstly, the fact that vehicles merge earlier into the roundabout seems to be partially caused by the way the overall traffic evolves. Note that, even though the initial state of the traffic configuration is the same in both cases, the decisions made in case 2 lead to a traffic scene where gaps are more evenly distributed, whereby incoming cars can find feasible merging gaps to target more easily. This conclusion comes from the fact that larger platoons of circulating vehicles, which do not split to accommodate any merging maneuver resulting in longer waiting times, are typically observed in case 1.

Interestingly, another advantage of case 2 over case 1 is that it mitigates problems related to the validity of the average acceleration assumption made to forecast the state of the vehicles delimiting the gap. If incoming vehicles only rely on certain gaps, they need to wait for large-enough and empty gaps to appear and for them to be able to accommodate a merging maneuver. When such gaps are found relatively far away (which in simulation was observed to happen often), the average-acceleration assumption—which is appropriate for rather short-term predictions—is not reliable enough. Consequently, situations where incoming cars commit first to a merging gap, and then find the gap infeasible when they are about to merge are sometimes observed (see for instance trajectory ① in Fig. 8, case 1). The fact that incoming vehicles

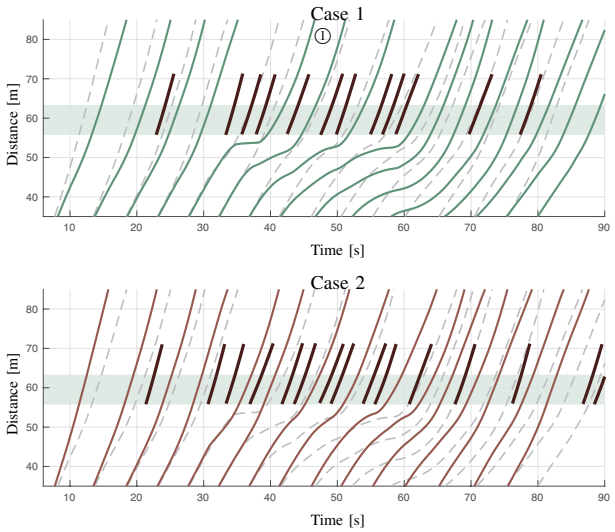

Fig. 8. Merging trajectories (green and red lines) of a set of vehicles on the same incoming lane. The same traffic scenario was used in both cases and the algorithm considers only certain gaps in case 1, and both certain and uncertain gaps in case 2. The part of the trajectories of the circulating vehicles that pass by the merging spot of the considered incoming lane are shown by the black lines. Merging trajectories are also shown in the complementary plot by the gray dashed lines. Finally, the region from the yield line to the merging spot is represented by the shaded area.

have a more optimistic view of the traffic scene in case 2, makes them target potential merging gaps that are closer and usually occupied by vehicles that are expected to exit, which constrains the acceleration that the vehicles at the limit of the gap can apply. That in turns improves the validity of the constant-acceleration assumption, and reduces the frequency of harsh stopping maneuvers.

The described phenomenon also suggests that a relatively straightforward improvement of the presented approach could be making vehicles that commit to far-away certain gaps, set up as well a safety constraint that allowed them to gently stop if the constant-acceleration assumptions happen not to well represent the real evolution of the traffic scene.

D. Aggregated effect

Finally, the aggregated effect of the proposed maneuver planner is assessed by evaluating the overall traffic coordination performance it leads to. Particularly three merging behaviors were compared: (behavior 1) a reactive merging behavior similar to the one formulated in §5-A in [5], (behavior 2) the proposed merging behavior, but only considering certain gaps, and (behavior 3) the proposed merging strategy in full.

A total of 2.2k simulations were carried out, varying the origin-destination pattern of the vehicles, the roundabout size, and the incoming traffic volume, as well as the confidence with which incoming vehicles guess the right destination of vehicles in the roundabout. Every single traffic scenario was simulated three times, one per considered merging behavior, and the vehicles' average travel speed distribution was saved and used as a traffic performance indicator.

Results are shown in Fig. 9, where simulations were grouped according to the merging behavior and the traffic

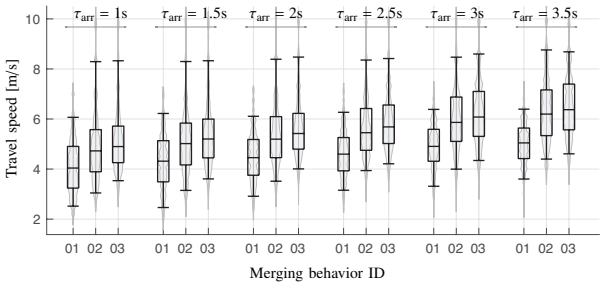

Fig. 9. Distribution of the vehicles' travel speed obtained from a set of 2.2k simulations for different incoming traffic density (given by the inter-vehicle arrival time interval τ_{arr}, for three different merging behaviors, and different driving intent prediction accuracy, roundabout size, origin-destination pattern, etc. Results are here grouped according to the incoming traffic density and the merging behaviors being compared.

inflow volume. That is, the average travel speed of all vehicles in cases matching a certain traffic inflow volume and a merging behavior ID have been aggregated and represented as box plots.

It can be seen that our reachability-based merging policy performs better than the reactive one used as the baseline, observing a relative improvement of about 21% between merging behaviors 2 and 1. Additionally, the positive impact that the explicit consideration of uncertain gaps (behavior 3) has on the merging trajectories gets as well reflected on the overall traffic performance, which further improves an additional 5% w.r.t. behavior 2.

Furthermore, it is worth pointing out that the reported relative improvement was averaged over the confidence with which vehicles are assumed to guess the right destination of the circulating cars. Slightly better/worse overall traffic coordination improvements can be expected for extremely good/bad driving intent predictions.

VI. Conclusions

In this work, a merging strategy to be used at SLRs has been presented. This merging strategy allows explicitly taking into account the probability with which vehicles in the circulatory lane are predicted to exit the intersection before the ego vehicle's merging spot, as well as the time at which the real intention of the nearby vehicles is expected to be revealed. The main feature of the algorithm is the formulation of the set of reachable merging targets, which enables planning merging trajectories that allow the vehicle to brake before a certain distance, during a certain time interval. This, in turn, allows characterizing the solution space for the targeted merging maneuver in an intuitive manner and without the need of explicitly generating any trajectory.

The proposed modular architecture has been shown to be computationally efficient and to generate smooth and safe merging trajectories that increase the overall traffic performance about 25% w.r.t. a simpler reactive policy.

The way our strategy handles uncertainty—expecting a certain improvement of the traffic state while always keeping a safe backup plan in case the expected traffic scene does not materialize—has been shown to bring benefits without compromising safety, and will be further explored in our future work.

The strategy is currently being extended to handle multi-lane roundabouts, and problems stemming from early merging commitments to certain gaps—a point discussed in §V—as well as occlusions.

VII. Acknowledgments

The investigations leading to the results shown herein were partially funded by the International *Chair Drive For All*.

References

[1] S. O.-R. A. V. S. Committee *et al.*, "Taxonomy and definitions for terms related to on-road motor vehicle automated driving systems," *SAE International*, 2014.

[2] J. Rios-Torres and A. A. Malikopoulos, "A survey on the coordination of connected and automated vehicles at intersections and merging at highway on-ramps," *IEEE Transactions on Intelligent Transportation Systems*, vol. 18, no. 5, pp. 1066–1077, 2017.

[3] W. Schwarting, J. Alonso-Mora, and D. Rus, "Planning and decision-making for autonomous vehicles," *Annual Review of Control, Robotics, and Autonomous Systems*, no. 0, 2018.

[4] G. R. de Campos, P. Falcone, R. Hult, H. Wymeersch, and J. Sjöberg, "Traffic coordination at road intersections: Autonomous decision-making algorithms using model-based heuristics," *IEEE Intelligent Transportation Systems Magazine*, vol. 9, no. 1, pp. 8–21, 2017.

[5] E. Debada and D. Gillet, "Virtual vehicle-based cooperative maneuver planning for connected automated vehicles at single-lane roundabouts," *IEEE Intelligent Transportation Systems Magazine*, vol. 10, no. ARTICLE, pp. 35–46, 2018.

[6] C. Burger and M. Lauer, "Cooperative multiple vehicle trajectory planning using miqp," in *2018 21st International Conference on Intelligent Transportation Systems (ITSC)*. IEEE, 2018, pp. 602–607.

[7] X. Qian, F. Altché, P. Bender, C. Stiller, and A. de La Fortelle, "Optimal trajectory planning for autonomous driving integrating logical constraints: An miqp perspective," in *2016 IEEE 19th International Conference on Intelligent Transportation Systems (ITSC)*. IEEE, 2016, pp. 205–210.

[8] E. Debada and D. Gillet, "Cooperative circulating behavior at single-lane roundabouts," in *2018 IEEE 21st International Conference on Intelligent Transportation Systems (ITSC)*. IEEE, 2018, pp. 3306–3313.

[9] J. Nilsson, M. Brännström, E. Coelingh, and J. Fredriksson, "Lane change maneuvers for automated vehicles," *IEEE Transactions on Intelligent Transportation Systems*, vol. 18, no. 5, pp. 1087–1096, 2017.

[10] C. Hubmann, J. Schulz, M. Becker, D. Althoff, and C. Stiller, "Automated driving in uncertain environments: Planning with interaction and uncertain maneuver prediction," *IEEE Transactions on Intelligent Vehicles*, vol. 3, no. 1, pp. 5–17, 2018.

[11] R. Schubert, "Evaluating the utility of driving: Toward automated decision making under uncertainty," *IEEE Transactions on Intelligent Transportation Systems*, vol. 13, no. 1, pp. 354–364, 2012.

[12] S. Ulbrich and M. Maurer, "Probabilistic online pomdp decision making for lane changes in fully automated driving," in *16th International IEEE Conference on Intelligent Transportation Systems (ITSC 2013)*. IEEE, 2013, pp. 2063–2067.

[13] W. Zhan, C. Liu, C.-Y. Chan, and M. Tomizuka, "A non-conservatively defensive strategy for urban autonomous driving," in *2016 IEEE 19th International Conference on Intelligent Transportation Systems (ITSC)*. IEEE, 2016, pp. 459–464.

[14] F. Damerow and J. Eggert, "Risk-aversive behavior planning under multiple situations with uncertainty," in *2015 IEEE 18th International Conference on Intelligent Transportation Systems*. IEEE, 2015, pp. 656–663.

[15] C. Pek, P. Zahn, and M. Althoff, "Verifying the safety of lane change maneuvers of self-driving vehicles based on formalized traffic rules," in *2017 IEEE Intelligent Vehicles Symposium (IV)*. IEEE, 2017, pp. 1477–1483.

[16] A. Rizaldi, F. Immler, and M. Althoff, "A formally verified checker of the safe distance traffic rules for autonomous vehicles," in *NASA Formal Methods Symposium*. Springer, 2016, pp. 175–190.